J Comput Aided Mol Des (2014) 28:265–276
DOI 10.1007/s10822-014-9727-1

Prediction of hydration free energies for the SAMPL4 diverse set of compounds using molecular dynamics simulations with the OPLS-AA force field

Oliver Beckstein · Anaïs Fourrier · Bogdan I. Iorga

Received: 16 November 2013 / Accepted: 3 February 2014 / Published online: 21 February 2014

Abstract All-atom molecular dynamics computer simulations were used to blindly predict the hydration free energies of a range of small molecules as part of the SAMPL4 challenge. Compounds were parametrized on the basis of the OPLS-AA force field using three different protocols for deriving partial charges: (1) using existing OPLS-AA atom types and charges with minor adjustments of partial charges on equivalent connecting atoms and derivation of new parameters for a number of distinct chemical groups (*N*-alkyl imidazole, nitrate) that were not present in the published force field; (2) calculation of quantum mechanical charges via geometry optimization, followed by electrostatic potential (ESP) fitting, using Jaguar at the LMP2/cc-pVTZ(-F) level; and (3) via geometry optimization and CHelpG charges (Gaussian09 at the HF/6-31G* level), followed by two-stage RESP fitting. The absolute hydration free energy was computed by an established protocol including alchemical free energy perturbation with thermodynamic integration. The use of standard OPLS-AA charges (protocol 1) with a number of newly parametrized charges and the use of histidine derived parameters for imidazole yielded an overall root mean square deviation of the prediction from the experimental data of 1.75 kcal/mol. The precision of our results appears to be mainly limited by relatively poor reproducibility of the Lennard-Jones contribution towards the solvation free energy, for which we observed large variability that could be traced to a strong dependence on the initial system conditions.

Keywords Molecular dynamics · Hydration free energy · OPLS-AA force field · Ligand parametrization · Free energy perturbation · Thermodynamic integration

Introduction

The change in Gibbs free energy for the transfer of a molecule from the gas phase to aqueous solution at constant temperature and pressure, the Gibbs hydration free energy ΔG_{hyd}, is an important quantity to describe and model the distribution of molecules in chemical and biological systems. It has also become a standard test case for the evaluation of the predictive power of quantitative computational methods, namely the SAMPL challenges [1–4]. Solvation free energies are also a key quantity in the parametrization of computational models such as classical additive force fields used in molecular mechanics [5–7] and serve as crucial benchmarks for the evaluation of existing force fields [8, 9].

In this SAMPL4 challenge [10] we employ classical all-atom molecular dynamics (MD) simulations in explicit solvent with additive and transferable force fields for the prediction of hydration free energies. Beyond the immediate task of accurately modelling small molecule-water interaction we are particularly interested in improving parameters for small and drug-like molecules so that their interactions with proteins are sufficiently well described to

Electronic supplementary material The online version of this article (doi:10.1007/s10822-014-9727-1) contains supplementary material, which is available to authorized users.

O. Beckstein (✉)
Department of Physics, Arizona State University,
P.O. Box 871504, Tempe, AZ 85287-1504, USA
e-mail: oliver.beckstein@asu.edu

A. Fourrier · B. I. Iorga (✉)
Institut de Chimie des Substances Naturelles, CNRS UPR 2301,
Centre de Recherche de Gif-sur-Yvette, Labex LERMIT,
1 Avenue de la Terrasse, 91198 Gif-sur-Yvette, France
e-mail: bogdan.iorga@cnrs.fr

be useful in computational drug design. Classical all-atom MD simulations have been shown to be capable of yielding precise predictions for hydration free energies [11] and current force fields are believed to be accurate to 1−2.5 kcal mol^{-1} for the prediction of hydration free energies of typical small organic molecules [12–20].

The data set provided for the SAMPL4 challenge consisted of a blind set (compounds **1**–**24**) and a supplementary set (**25**–**52**) (Fig. 1) [21]. The blind set consisted of a diverse set of small molecules whose hydration free energies had not been published but were known to the SAMPL4 organizers. Hydration free energies for the supplementary set exist in the literature or could be calculated from literature data. In our study we treated both sets in the same manner and blindly predicted hydration free energies for all 52 compounds.

We used a windowed alchemical free energy perturbation approach to compute the hydration energy from the interactions between the solute and water. Interactions were parametrized on the basis of the OPLS-AA force field [6, 22–35]. Electrostatic interactions between solute and water typically dominate the solvation free energy. The OPLS-AA force field philosophy prescribes that atomic partial charges are initially determined for small model compounds. These charge can be directly transferred to an atom in another molecule that experiences the same chemical environment as the atom in the model compound. Thus, an OPLS-AA atom type is characterized by both its Lennard-Jones potential parameters and its fixed partial charge. Therefore, OPLS-AA contains a much large number of atom types than other force fields, which typically generate partial charges on a per-molecule basis. One possible advantage of rich, fine-grained atom typing is the relative ease with which new molecules can be parametrized using chemical rules. Within the SAMPL4 challenge we tried to answer the question of how the transferable partial charge assignment philosophy in OPLS-AA compares to non-transferable charges based on *ab-initio* quantum mechanical (QM) calculations. To this end we tested three different protocols P1–P3 for generating atomic partial charges. Protocol P1 employed native OPLS-AA charges whereas protocols P2 and P3 computed the charges at the QM level for each compound with two different methods.

Methods

Chemical structures **1**–**52** were converted from SMILES format to PDB format with CORINA version 3.44 (http://www.molecular-networks.com). MD trajectories were analyzed with Gromacs tools (http://www.gromacs.org) [36] and MDAnalysis [37]. The OPLS-AA force field files that are part of Gromacs 4.5.5 [36] were used as a basis for the parametrization of all compounds. Topologies were generated using the MOL2FF algorithm developed by our groups (manuscript in preparation). The MOL2FF tool is based on the CACTVS Chemoinformatics Toolkit (http://www.xemistry.com/) and is thus "chemically-aware" so that it can automatically assign OPLS-AA atom types based on the chemical function. The hydration free energy depends strongly on the partial charges and hence three different protocols P1–P3 were tested for charge generation. We considered the use of these three protocols since we previously showed [20] that in some cases P2 and P3 outperform P1 (which is based on the the standard OPLS-AA charges, see below). However, the charges from P2 and P3 are not transferable to other compounds containing similar chemical functions, but they can be useful for the parametrization of new OPLS-AA atom types with transferable charges [20]. The Lennard-Jones and bonded interactions were kept the same for protocols P1 to P3.

P1: OPLS-AA charges For parametrization protocol P1, the native charges from OPLS-AA were used. When these were missing, they were parametrized using experimental hydration free energy data available (see below).

P2: LMP2/cc-pVTZ(-F) QM charges For protocol P2, the charges were obtained after geometry optimization and electrostatic potential (ESP) fitting, using Jaguar (http://www.schrodinger.com) at the LMP2/cc-pVTZ(-F) level. This methodology has been previously used for the OPLS-AA force field development (protein amino acids and small organic molecules) [23, 28, 29]. The charges for chemically equivalent atoms obtained from the Jaguar calculations output were generally not identical, and they were adjusted manually before further use.

P3: HF/6-31G QM charges* For P3, the charges were obtained after geometry optimization and CHelpG charges calculation using Gaussian09 (http://www.gaussian.com) [38] at the HF/6-31G* level, then a two-stage RESP fitting using AmberTools (http://ambermd.org). This methodology has been previously used for heterocycles parameterization in the OPLS-AA force field [25, 26].

Hydration free energy calculation

Hydration free energies were calculated as described previously [20] via alchemical free energy perturbation (FEP) MD simulations of each molecule in a water box. All simulations were performed with Gromacs 4.5.5 [36]. Each molecule was solvated with TIP4P water [39] in a dodecahedral periodic simulation cell with at least 1.0 nm between the solute and the box surfaces, then an equilibrium simulation at constant temperature and pressure ($T = 300$ K, $P = 1$ bar) was carried out for 10 ns. The simulations were run as Langevin dynamics (integration

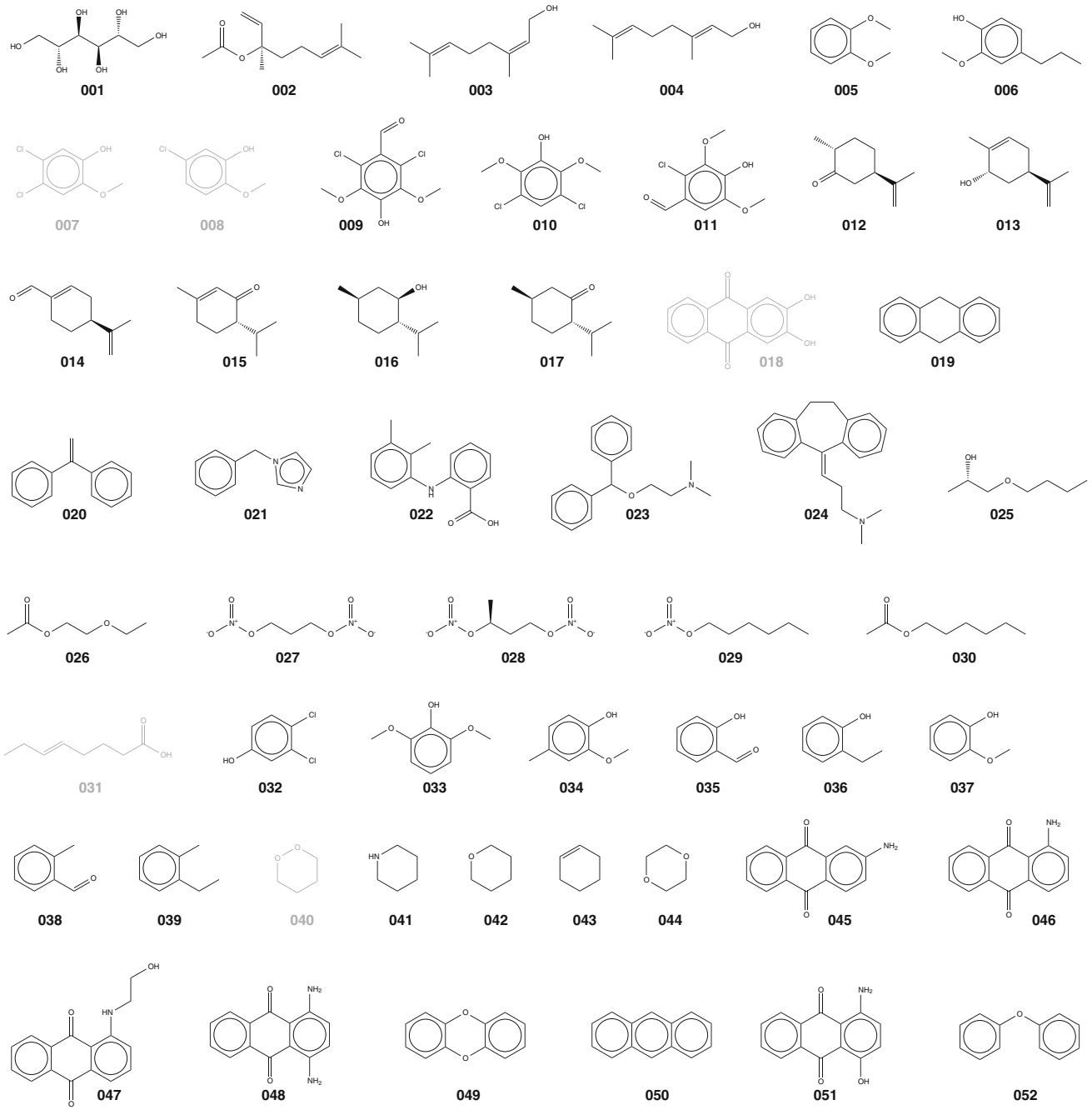

Fig. 1 Chemical structures of the compounds from the SAMPL4 data set. Compounds **1**–**24** constitute the blind set and **25**–**52** comprise the supplementary set. **7**, **8**, **18**, **31** and **40** were removed from the final data set by the SAMPL4 organizers and are represented in *gray*

time step 2 fs) for temperature control, with the friction coefficient for each particle computed as mass/0.1 ps. The average pressure was held constant with an isotropic Berendsen barostat (relaxation time constant $\tau_p = 1$ ps and compressibility $\kappa_T = 4.6 \times 10^{-5}$ bar^{-1}). The grid-based neighbor list was updated every five time steps. Lennard-Jones interactions were calculated up to a cutoff of 1 nm and a dispersion correction (implemented in Gromacs) was applied to energy and pressure to account for van der Waals interactions beyond the cutoff in a mean field manner [40]. Coulomb interactions were handled with the SPME method [41] (short range cutoff 1 nm, 0.12 nm Fourier grid spacing, sixth order spline interpolation, relative tolerance 10^{-6}). Bonds containing hydrogen atoms were constrained with the P-LINCS algorithm [42] (fourth order expansion with a single iteration). The last frame of the *NPT* simulation was used as the input for the FEP simulations. FEP calculations were performed in the *NVT*

ensemble without a barostat but used the same parameters as the *NPT* simulations with the exception of FEP specific alterations and a higher P-LINCS matrix expansion order of 12. Coulomb interactions (partial charges) were linearly switched off over five windows (coupling parameter $\lambda_{\text{Coul}} \in \{0, 0.25, 0.5, 0.75, 1\}$) while the van der Waals (Lennard-Jones) interactions were maintained (i.e. $\lambda_{\text{vdW}} = 0$); sixteen windows were used to switch off the Lennard-Jones term for the uncharged solute ($\lambda_{\text{Coul}} = 1$ and $\lambda_{\text{vdW}} \in$ {0, 0.05, 0.1, 0.2, 0.3, 0.4, 0.5, 0.6, 0.65, 0.7, 0.75, 0.8, 0.85, 0.9, 0.95, 1}). Each window was simulated for 5 ns. The van der Waals calculations used soft core potentials with the values suggested by Mobley [12] ($\alpha = 0.5$, power 1, and $\sigma = 0.3$ nm). The calculations made use of the "`couple-intramol = no`" feature in Gromacs [36], which maintains intramolecular interactions while decoupling all intermolecular ones. Helmholtz free energies and statistical errors for the discharging and decoupling process were calculated with thermodynamic integration (TI)

$$\Delta A = \int_0^1 \left\langle \frac{\partial \mathscr{H}}{\partial \lambda} \right\rangle d\lambda, \tag{1}$$

over the averaged derivative of the Hamiltonian with respect to the coupling parameter λ, $\partial \mathscr{H}/\partial \lambda$, as described previously [20]. $\partial \mathscr{H}/\partial \lambda$ was saved for every time step (1 ps). Eq. 1 was integrated with the composite Simpson's rule [43] as implemented in SciPy (http://www.scipy.org). The error on the hydration free energy was estimated from the errors of the individual $\langle \partial \mathscr{H}/\partial \lambda \rangle$ of each FEP window. The error δ of the mean $\langle \partial \mathscr{H}/\partial \lambda \rangle$ was calculated as

$$\delta = \sqrt{2 t_c C(0) \tau^{-1}} \tag{2}$$

where $C(t)$ is the autocorrelation function of the fluctuations around the mean ($\partial \mathscr{H}/\partial \lambda - \langle \partial \mathscr{H}/\partial \lambda \rangle$), t_c the correlation time (assuming an inital exponential decay of the autocorrelation function $C(t) \sim \exp(-t/t_c)$), and τ the total length of the simulation [44]. The error on each TI integral was calculated analytically via propagation of errors through Simpson's rule. The final error on ΔA_{hyd} was thus $(\delta^2_{\text{Coul}} + \delta^2_{\text{vdW}})^{1/2}$. The total hydration free energy (transfer from gas phase to aqueous phase at the 1M/1M Ben-Naim standard state) was calculated as $\Delta A_{\text{hyd}} = -(\Delta A_{\text{Coul}} + \Delta A_{\text{vdW}})$. We are directly comparing computed Helmholtz free energies of hydration to experimental Gibbs free energies because the difference in free energy between ΔG_{hyd} and ΔA_{hyd} is only on the order of 0.1 kcal/mol for the systems simulated here as judged from a thermodynamic analysis of cavity formation (O. Beckstein, unpublished).

In some cases, for simulations of the same compound using the charges generated with protocols P1–P3, we observed relatively poor reproducibility of the Lennard-Jones contribution ΔA_{vdW} towards the solvation free energy (see Supplementary Information file for a detailed presentation of the computed hydration free energy results). Such behavior was somewhat unexpected since the Lennard-Jones parameters are identical for all simulations of the same compound and only the partial charges and hence the Coulomb contribution was expected to differ substantially. After the SAMPL4 challenge, we carried out a number of additional simulations to better understand under which circumstances ΔA_{vdW} was reproducible, as reported below.

Parametrization of missing OPLS-AA parameters

Force field parameters were not available for *N*-substituted imidazoles (compound **21**), alkyl nitrates (compounds **27**–**29**) and peroxides (compound **40**) in the original OPLS-AA force field, and these parameters were generated as described below. However, as the compound **40** was discarded from the final data set by the SAMPL4 organizers, the OPLS-AA parametrization of the peroxide group will not be described here. When necessary, missing angle and dihedral bonding parameters were obtained in a manner similar with the published OPLS-AA protocol [23].

N-Substituted imidazoles

We started by computing the hydration free energy for the simplest imidazole-containing chemical group available in the OPLS-AA force field, the imidazole itself (**53** in Fig. 2), using two different sets of charges. Table 1 shows that the imidazole parameters from histidine provide a better agreement with the available experimental values [1, 14, 45] (<1 kcal mol^{-1} unsigned error) than those originally present in the OPLS-AA force field. The calculated van der Waals term is practically the same in both cases, and the difference between these two value is solely due to the Coulomb term.

In the next step, the hydration free energy was computed for *N*-methyl imidazole (**54**), using the same two sets of charges as before and, in each case, two different approaches to incorporate the charge of the hydrogen

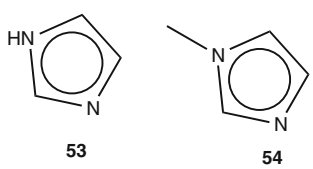

Fig. 2 Chemical structures of imidazole **53** and *N*-methyl imidazole **54** used for the OPLS-AA parametrization of *N*-substituted imidazoles

atom replaced by the methyl group: this supplementary charge was added either on the endocyclic nitrogen atom bearing the methyl group or on the exocyclic carbon atom from the methyl group. Calculations were also carried out using non-transferable parameters obtained with protocols P2 and P3 (see Table 1). The parameters with charge modified on the exocyclic carbon atom reproducibly give the best results (Table 1, entries 4 and 6) and among them, as already noticed above, the imidazole OPLS-AA parameters taken from histidine give the closest value to the experimental one [14], with an unsigned error of 0.3 kcal mol^{-1} (Table 1, entry 6). These last parameters were then used for the parametrization of compound **21**, with an additional modification of the charge on the exocyclic carbon atom to take into account the influence of the phenyl group.

Nitrates

In the first step, we calculated the partial charges for the two simplest alkyl nitrates, methyl nitrate **55** and ethyl nitrate **56** (Fig. 3), using the protocols P2 and P3. This provided initial estimates for the magnitude of these charges and how they are influenced by the substitution in the α position. The results in Table 2 show that most of the atoms are influenced by this substitution, with the notable exception of the nitrogen and oxygen atoms of the NO_2 group. In order to limit the number of new OPLS-AA force field parameters to be introduced and given the chemical similarity and the relatively good partial charge compatibility, we decided to use the ester OPLS-AA parameters for the 'RO' fragment of alkyl nitrates (opls_467 for oxygen, opls_468 for carbon and opls_469 for α hydrogen atoms), and to derive new parameters for the 'NO_2' fragment, using the nitro group parameters as a starting point. Six transferable trial charge sets C1–C6 were defined (Table 2), containing fixed charges for the 'RO' fragment and variable charges for the 'NO_2' fragment. C1–C6 were tested for their ability to reproduce experimental values for the hydration free energy.

We were able to identify from the literature six alkyl mono- and dinitrates for which experimental hydration free energy values were available, none of them being present in the SAMPL4 data set. The compounds **57–62** (Fig. 3) were then selected for further evaluation. In Table 3 we compare the experimental and computed values of hydration free energy for these compounds. The charge set C5 was able to reproduce the experimental values for alkyl mononitrates **57–60** very well (unsigned error of <0.5 kcal mol^{-1}). Charge set C6 appeared better suited for the alkyl dinitrates **61** and **62**. However, in order to provide a single charge set to be used for all nitrates, the C5 charge set was selected and subsequently used for the simulations of compounds **27–29**.

Results and discussion

The two main results of our study are validated new OPLS-AA atom types for *N*-substituted imidazoles and alkyl nitrates and an evaluation of the accuracy of transferable OPLS-AA charges in comparison to non-transferable QM-derived partial charges.

Parametrization and validation of new OPLS-AA atom types

The new OPLS-AA atom-types generated during this study are presented in Table 4. They were validated by comparison of experimental and computed hydration free energies values, which showed unsigned errors <1 kcal mol^{-1} for unsubstituted imidazole **53**, 0.3 kcal mol^{-1} for *N*-methyl imidazole **54** (Table 1) and <0.5 kcal mol^{-1} for alkyl mononitrates (**29** in Table 5 and **57–60** in Table 3). However, for *N*-benzyl imidazole **21** (Table 5) and for alkyl dinitrates **27**, **28**, **61** and **62** (Tables 5 and 3) much higher unsigned errors (> 2 kcal mol^{-1}) were observed. In the latter case the results are likely the consequence of the use of C5 charge set (see Table 2) that is more compatible with alkyl mononitrates than with dinitrates. The former result was unanticipated because the hydration free energy for the smaller fragments of *N*-benzyl imidazole **21**, namely toluene and *N*-methyl imidazole, are very well reproduced by the OPLS-AA force field. We are currently investigating this issue.

Predicted hydration free energies

For each molecule, hydration free energy calculations were carried out using the three topologies generated with protocols P1–P3. The corresponding three sets of results ($\Delta A^{(1)}_{hyd}$ to $\Delta A^{(3)}_{hyd}$ in Table 5) were submitted to the SAMPL4 challenge. The accuracy of the computed hydration free energies was quantified by computing the root mean square error (RMSE) from the experimental hydration free energies ΔG^{exp}_{hyd} published after the conclusion of SAMPL4 (Table 5).

The native, transferable OPLS-AA parameters (P1) produced much better agreement with experiment than the non-transferable *ab-initio* charges (Fig. 4), with an R^2 correlation coefficient of 0.84 compared to 0.61 for P2 and P3. P1 also better described the relative ordering of compounds as judged from a higher Kendall's tau rank correlation coefficient (τ) of 0.70 compared to 0.51 for P2 and 0.43 for P3.

Table 1 Computed (ΔA_{hyd}) *vs* experimental (ΔG^{exp}_{hyd}) hydration free energy values for imidazole **53** and *N*-methyl imidazole **54** in kcal mol^{-1}

Id	ΔG^{exp}_{hyd}	Ref	ΔA_{hyd}	$\Delta A_{Coulomb}$	ΔA_{vdW}	Charges
53	−9.81 ··· −9.63	[1, 14, 45]	−7.70(4)	8.23(2)	−0.52(4)	OPLS-AA imidazole
			−8.81(5)	9.30(2)	−0.49(4)	OPLS-AA histidine
54	−8.41	[14]	−3.84(5)	4.92(2)	−1.08(4)	OPLS-AA imidazole, charge modified on N
			−7.18(5)	8.19(2)	−1.01(5)	OPLS-AA imidazole, charge modified on C
			−6.27(5)	6.94(2)	−0.66(4)	OPLS-AA histidine, charge modified on N
			−8.71(5)	9.55(3)	−0.84(4)	OPLS-AA histidine, charge modified on C
			−9.12(5)	9.66(3)	−0.55(4)	P2
			−6.30(5)	7.39(2)	−1.09(4)	P3

The Coulomb and van der Waals contributions to ΔA_{hyd} are also shown. The standard error in the last significant digits is given in parentheses

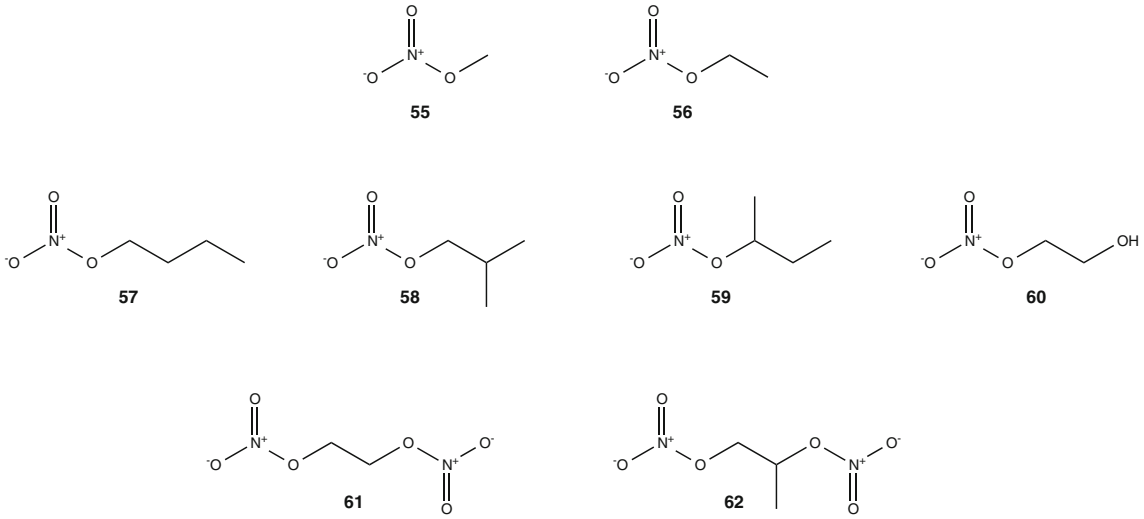

Fig. 3 Chemical structures of alkyl mono- (**55–60**) and di-nitrates (**61**, **62**) used for the OPLS-AA parametrization of the nitrate group

Taking only those compounds into account for which SAMPL4 provided accurate experimental data (compounds **1–6**, **9–17**, **19–30**, **31–39**, **41–52**), the overall RMSE for the OPLS-AA (P1) calculations was 1.75 kcal mol^{-1}. The non-transferable charge sets showed substantially worse agreement with 2.50 kcal mol^{-1} (P2) and 2.76 kcal mol^{-1} (P3), as seen in Table 5. Notably, for all three approaches, the agreement between predicted and experimental free energies was similar across the blind and the supplementary data set, with variations in RMSE of 0.43 kcal mol^{-1} between data sets. Thus, our parametrization do not appear to be inherently biased towards compounds for which hydration free energies are already known. Hydration free energies for compounds for which we had to parametrize atom types to be used in protocol P1 (**21**, **27–29**) were predicted to a similar level of accuracy as compounds for which published OPLS-AA atom types were available (Fig. 4).

Table 2 Partial charges for methyl nitrate **55** and ethyl nitrate **56** computed with protocols P2 and P3, and transferable trial charge sets C1–C6 for hydration free energy calculations of alkyl nitrates (see Table 3)

Id	R	H(C)	C	O(C)	N	O(=N)	Charge set
55		0.097	0.016	−0.308	0.843	−0.421	P2
		0.084	0.052	−0.374	1.046	−0.488	P3
56	−0.039	0.016	0.428	−0.395	0.840	−0.434	P2
	−0.025	−0.011	0.418	−0.429	1.041	−0.492	P3
		0.030	0.160	−0.330	1.100	−0.510	C1
		0.030	0.160	−0.330	1.050	−0.485	C2
		0.030	0.160	−0.330	1.000	−0.460	C3
		0.030	0.160	−0.330	0.950	−0.435	C4
		0.030	0.160	−0.330	0.900	−0.410	**C5**
		0.030	0.160	−0.330	0.850	−0.385	C6

Ultimately, C5 was selected to represent all nitrates

Protocol P1, the standard OPLS-AA parameters with the addition of our new atom types, performed better than the non-transferrable *ab-initio* charges (protocols P2 and P3). In the previous SAMPL3 challenge, P3 produced the best results because it turned out that OPLS-AA was missing specific chloro-substituent parameters [20]. We interpret the relative success of the native OPLS-AA atom types to mean that the chemical space of the SAMPL4 compounds was more evenly covered by the available OPLS-AA parameters. It is encouraging that transferable OPLS-AA parameters provide reasonably accurate predictions of solvation free energies if appropriate atom types already exist. We previously showed for the case of a more restricted set of chlorinated compounds that a simple introduction of a new atom type for chloro-substituents could improve the accuracy of standard OPLS-AA from 2.4 kcal mol^{-1} to 1.0 kcal mol^{-1} RMSE compared to experiment [20]. The value in performing hydration free energy calculations with non-transferable *ab-initio* charges lies in the fact that cases when transferable OPLS-AA atom types are missing can be detected and new atom types can be introduced using these charges as a starting point [20]. It appears that classical transferable force fields such as OPLS-AA can be made accurate for water-solute

Table 3 Experimental and computed hydration free energy values (in kcal mol^{-1}) for nitrates **57**-**62**, using the charge sets C1–C6 from Table 2

Id	ΔG_{hyd}^{exp}	Ref	ΔA_{hyd}	ΔA_{Coul}	ΔA_{vdW}	Charge set
57	−2.09 ··· −2.10	[2, 45]	−3.51(5)	5.12(2)	−1.61(5)	C1
			−3.93(5)	4.56(2)	−0.63(5)	C2
			−2.51(5)	4.06(1)	−1.56(5)	C3
			−2.46(6)	3.62(1)	−1.16(5)	C4
			−1.90(5)	3.21(1)	−1.31(5)	**C5**
			−1.65(5)	2.86(1)	−1.21(5)	C6
58	−1.88 ··· −1.90	[2, 45]	−4.18(5)	4.97(2)	−0.79(5)	C1
			−3.24(5)	4.52(2)	−1.27(5)	C2
			−2.71(5)	4.05(1)	−1.34(5)	C3
			−2.52(5)	3.58(1)	−1.06(5)	C4
			−1.91(5)	3.17(1)	−1.26(5)	**C5**
			−1.08(5)	2.82(1)	−1.74(5)	C6
59	−1.80 ··· −1.82	[2, 45]	−3.74(5)	4.93(2)	−1.19(5)	C1
			−2.67(5)	4.44(1)	−1.77(5)	C2
			−2.82(5)	3.95(1)	−1.13(5)	C3
			−1.73(5)	3.52(1)	−1.79(5)	C4
			−1.36(5)	3.12(1)	−1.75(5)	**C5**
			−0.96(5)	2.78(1)	−1.82(5)	C6
60	−8.18 ··· −8.20	[2, 45]	−9.80(5)	10.41(3)	−0.61(5)	C1
			−9.20(5)	9.92(3)	−0.72(5)	C2
			−8.61(5)	9.46(3)	−0.86(5)	C3
			−7.84(5)	9.12(3)	−1.28(5)	C4
			−7.67(5)	8.70(3)	−1.03(5)	**C5**
			−7.40(5)	8.34(3)	−0.95(4)	C6
61	−5.70 ··· −5.73	[2, 45]	−10.11(6)	10.17(3)	−0.06(5)	C1
			−8.70(6)	9.11(3)	−0.41(5)	C2
			−8.19(6)	8.12(3)	0.07(5)	C3
			−7.23(6)	7.38(3)	−0.15(5)	C4
			−6.37(6)	6.54(2)	−0.17(5)	**C5**
			−6.02(5)	5.90(2)	0.12(5)	C6
62	−4.95 ··· −5.00	[2, 45]	−9.92(7)	9.96(3)	−0.05(6)	C1
			−8.62(6)	9.08(2)	−0.46(6)	C2
			−7.92(7)	8.05(2)	−0.13(6)	C3
			−7.19(7)	7.29(2)	−0.10(6)	C4
			−5.93(6)	6.54(2)	−0.60(6)	**C5**
			−5.22(6)	5.90(2)	−0.68(6)	C6

C5 was considered the best compromise for representing both mono- and di-nitrates. The standard error in the last significant digits is given in parentheses

interactions to about 1.5 kcal mol^{-1} by relatively small and localized adaptations. Similar strategies have been adopted to more accurately model cation-π interactions in the CHARMM force field, which enabled the identification of specific protein-drug interactions for a number of allosteric modulators of a class A GPCR, the M2 muscarinic receptor [46].

Reproducibility of the van der Waals contribution to the free energy

We observed that the van der Waals contribution ΔA_{vdW} for protocols P1, P2, and P3 could vary by a few kcal/mol (Table S1), even though the protocols only differed by the partial charge assignment and hence in principle only the Coulomb contribution ΔA_{Coul} should have varied substantially. We investigated this behavior for selected compounds **5**, **22**, **23**, and **44**, which showed relatively high unsigned errors for ΔA_{hyd} (Table 5). The FEP simulations for all three protocols were repeated with a length of 10 ns per FEP window instead of 5 ns (entries "B" in Table S2). These simulations used the same starting conformation as the simulations "A", which are the same as reported in Table 5. In all cases, both the Coulomb and the van der Waals term are fully reproducible to within <0.1 kcal mol^{-1} (comparable to the statistical errors computed from the FEP windows themselves) and thus they do not seem to be dependent on the length of FEP windows. An additional set of simulations ("C") was performed in which the initial *NPT* equilibrium simulation was also repeated. Therefore, the FEP windows (run length 10 ns each) were initialized from a different conformation than the previously described simulations. For the three protocols, ΔA_{vdW} differed between "B" and "C" by between 0.55 and 1.87 kcal mol^{-1} while ΔA_{Coul} was much less affected (Table S2).

Thus, our simulations clearly show that the hydration free energies (and in particular the van der Waals contributions) are fully reproducible provided that the initial conformation considered for the FEP calculations is identical. Different starting frames, as used for the different protocols, which each performed their own equilibrium MD, lead to large variations in the van der Waals term. It is possible that by choosing the last frame of the *NPT* simulation for the FEP *NVT* simulations far from the equilibrium volume V_0 an error is introduced. In our case, the largest relative deviation from V_0 was 2.7% although the unsigned mean average 0.5% was much smaller (the average V_0 over all equilibrium simulations was 16.2nm^3 with a standard deviation of 3.1nm^3). However, we did not find an obvious correlation between the van der Waals terms and the deviations from V_0. Another possible source of heterogeneity is the conformational flexibility of the solute. An initial analysis in terms of solute conformers showed that small and rigid compounds (e.g. **44**) present the same initial conformation for all "A", "B" and "C" FEP calculations (Table S2). For bigger and more flexible compounds (e.g. **22**) we identified different initial conformations for the simulations "A"/"B" and "C" with the protocols P1–P3, and in this case the variability of the ΔA_{vdW} term could be the result of the two factors mentioned above. We are currently investigating how to separate multiple sources of heterogeneity in order to improve

Table 4 New OPLS-AA parameters for *N*-substituted imidazoles and alkyl nitrates

Name[a]	Type[b]	Z[c]	*m* (u)[d]	*q* (*e*)[e]	σ (nm)[f]	ε (kJ mol^{-1})[g]	
opls_146A	HA	1	1.008	−0.177	0.242	0.125520	H on CG in histidine-derived imidazole parameters
opls_135A	CT	6	12.011	0.146	0.350	0.276144	C in N–**C**H$_3$ substituted imidazoles with histidine-derived parameters
opls_136A	CT	6	12.011	0.206	0.350	0.276144	C in N–**C**H$_2$R substituted imidazoles with histidine-derived parameters
opls_136B	CT	6	12.011	0.321	0.350	0.276144	C in N–**C**H$_2$Ph substituted imidazoles with histidine-derived parameters
opls_137A	CT	6	12.011	0.266	0.350	0.276144	C in N–**C**HR$_2$ substituted imidazoles with histidine-derived parameters
opls_139A	CT	6	12.011	0.326	0.350	0.276144	C in N–**C**R$_3$ substituted imidazoles with histidine-derived parameters
opls_760A	NO	7	14.0067	0.900	0.325	0.502080	R–O**N**O$_2$ alkyl nitrates
opls_761A	ON	8	15.9994	−0.410	0.296	0.711280	R–ON**O**$_2$ alkyl nitrates

[a] Proposed OPLS-AA atom type name

[b] Bonded type

[c] Atomic number

[d] Atomic mass in atomic mass constants $m_u = 1.660538921 \times 10^{-27}$ kg

[e] Partial charge in elementary charges $e = 1.602176565 \times 10^{-19}$ C

[f] Length parameter of the OPLS-AA Lennard-Jones potential $V_{LJ}(r) = 4\varepsilon[(\sigma/r)^{12} - (\sigma/r)^6)]$ [6]

[g] Energy well depth of the OPLS-AA Lennard-Jones potential $V_{LJ}(r)$

Table 5 Computed (ΔA_{hyd}) and experimental hydration free energies (ΔG_{hyd}) with error estimate (in kcal mol^{-1}) for all SAMPL4 compounds (denoted by "id")

Id	Exp.	Protocol 1		Protocol 2		Protocol 3	
	ΔG_{hyd}^{exp}	$\Delta A_{hyd}^{(1)}$	$D^{(1)}$	$\Delta A_{hyd}^{(2)}$	$D^{(2)}$	$\Delta A_{hyd}^{(3)}$	$D^{(3)}$
1	−23.62(32)	−20.04(28)	3.58	−16.29(11)	7.33	−20.02(14)	3.60
2	−2.49(85)	−1.52(8)	0.97	−3.86(9)	1.37	−4.14(8)	1.65
3	−4.78(25)	−2.68(8)	2.10	−2.72(8)	2.06	−3.90(7)	0.88
4	−4.45(24)	−2.66(8)	1.79	−2.77(8)	1.68	−3.11(7)	1.34
5	−5.33(10)	−2.97(6)	2.36	−3.72(6)	1.61	−3.10(6)	2.23
6	−5.26(18)	−2.96(7)	2.30	−6.06(7)	0.80	−2.53(7)	2.73
7		−5.14(7)		−3.16(7)		−3.31(7)	
8		−4.19(7)		−4.18(6)		−3.10(6)	
9	−8.24(76)	−10.42(9)	2.18	−10.84(10)	2.60	−10.49(9)	2.25
10	−6.24(38)	−6.11(8)	0.13	−4.62(8)	1.62	−5.74(8)	0.50
11	−7.78(77)	−8.70(9)	0.92	−7.88(9)	0.10	−8.57(8)	0.79
12	−3.75(21)	−2.74(7)	1.01	−6.49(8)	2.74	−4.56(7)	0.81
13	−4.44(43)	−4.27(8)	0.17	−5.41(8)	0.97	−5.08(7)	0.64
14	−4.09(17)	−2.31(7)	1.78	−4.45(7)	0.36	−3.67(7)	0.42
15	−4.51(10)	−3.05(7)	1.46	−6.64(7)	2.13	−5.75(7)	1.24
16	−3.20(27)	−4.38(8)	1.18	−4.20(7)	1.00	−4.86(8)	1.66
17	−2.53(25)	−2.61(7)	0.08	−4.36(7)	1.83	−4.22(7)	1.69
18		−12.44(9)		−15.74(9)		−14.84(10)	
19	−3.78(10)	−4.30(8)	0.52	−4.11(9)	0.33	−0.61(8)	3.17
20	−2.78(10)	−1.80(8)	0.98	−3.47(8)	0.69	−0.56(8)	2.22
21	−7.63(12)	−9.86(7)	2.23	−10.39(7)	2.76	−6.50(7)	1.13
22	−6.78(10)	−11.16(9)	4.38	−10.92(16)	4.14	−7.08(11)	0.30
23	−9.34(62)	−6.34(11)	3.00	−5.81(10)	3.53	−0.97(10)	8.37
24	−7.43(60)	−5.86(11)	1.57	−5.15(11)	2.28	−1.57(10)	5.86
RMSE blind subset			1.98		2.54		2.81
25	−5.73(15)	−3.72(8)	2.01	−2.55(9)	3.18	−3.60(7)	2.13
26	−5.31(10)	−4.07(7)	1.24	−6.17(6)	0.86	−6.92(6)	1.61
27	−4.80(39)	−7.10(6)	2.30	−10.10(6)	5.30	−10.94(6)	6.14
28	−4.29(39)	−6.91(6)	2.62	−10.18(7)	5.89	−10.08(6)	5.79
29	−1.66(10)	−1.46(6)	0.20	−3.22(6)	1.56	−5.25(6)	3.59
30	−2.29(12)	−0.53(7)	1.76	−4.80(7)	2.51	−4.21(7)	1.92
31		−3.78(6)		−6.11(7)		−7.21(7)	
32	−7.29(10)	−5.39(6)	1.90	−4.71(6)	2.58	−5.61(7)	1.68
33	−6.96(10)	−6.11(7)	0.85	−6.74(7)	0.22	−5.74(7)	1.22
34	−5.80(10)	−4.40(7)	1.40	−4.15(7)	1.65	−2.99(6)	2.81
35	−4.68(10)	−6.46(6)	1.78	−8.52(6)	3.84	−9.53(6)	4.85
36	−5.66(10)	−4.41(6)	1.25	−6.14(6)	0.48	−3.48(6)	2.18
37	−5.94(10)	−4.14(6)	1.80	−4.34(6)	1.60	−3.51(6)	2.43
38	−3.93(10)	−3.37(6)	0.56	−5.54(7)	1.61	−5.22(6)	1.29
39	−0.85(10)	−1.19(7)	0.34	−1.81(6)	0.96	0.46(6)	1.31
40		−2.78(5)		−4.07(5)		−3.47(5)	
41	−5.05(10)	−3.46(6)	1.59	−2.94(5)	2.11	−2.18(5)	2.87
42	−3.13(10)	−1.80(5)	1.33	−2.37(5)	0.76	−2.42(5)	0.71
43	0.14(10)	1.09(5)	0.95	0.55(5)	0.41	0.74(5)	0.60
44	−5.08(10)	−2.29(5)	2.79	−3.81(5)	1.27	−4.14(5)	0.94
45	−11.53(29)	−10.10(9)	1.43	−16.48(9)	4.95	−13.94(9)	2.41
46	−9.44(74)	−9.65(9)	0.21	−11.24(9)	1.80	−11.42(10)	1.98
47	−14.21(1.10)	−14.13(11)	0.08	−11.08(11)	3.13	−13.58(11)	0.63
48	−11.85(35)	−12.38(9)	0.53	−12.09(9)	0.24	−14.14(9)	2.29
49	−3.16(10)	−1.39(7)	1.77	−3.90(8)	0.74	−1.80(7)	1.36

Table 5 continued

Id	Exp.	Protocol 1		Protocol 2		Protocol 3	
	$\Delta G_{\mathrm{hyd}}^{\mathrm{exp}}$	$\Delta A_{\mathrm{hyd}}^{(1)}$	$D^{(1)}$	$\Delta A_{\mathrm{hyd}}^{(2)}$	$D^{(2)}$	$\Delta A_{\mathrm{hyd}}^{(3)}$	$D^{(3)}$
50	−4.14(10)	−3.11(7)	1.03	−3.93(7)	0.21	−1.00(8)	3.14
51	−9.53(28)	−11.35(10)	1.82	−10.34(10)	0.81	−12.32(11)	2.79
52	−2.87(69)	−0.92(7)	1.95	−2.93(8)	0.06	−1.66(8)	1.21
RMSE supplementary subset			1.55		2.47		2.71
RMSE global			1.75		2.50		2.76
Kendall's tau rank correlation coefficient (τ)		0.70		0.51		0.43	
Coefficient of determination (R^2)		0.84		0.61		0.61	

The hydration free energies were computed at constant volume (Helmholtz solvation free energies). The absolute difference between computed and experimental hydration free energy is shown for each compound and parametrization protocol i as $D_{\mathrm{id}}^{(i)} = |\Delta A_{\mathrm{hyd,id}}^{(i)} - \Delta G_{\mathrm{hyd,id}}^{\mathrm{exp}}|$. The standard error in the last significant digits is given in parentheses. The root mean square error (RMSE) $\sqrt{N^{-1}\sum_{\mathrm{id}}^{N} D_{\mathrm{id}}^2}$ is listed for the blind and supplementary subsets, as well as for the entire SAMPL4 data set (see text). For compounds **7**, **8**, **18**, **31**, and **40** no reliable experimental data were available

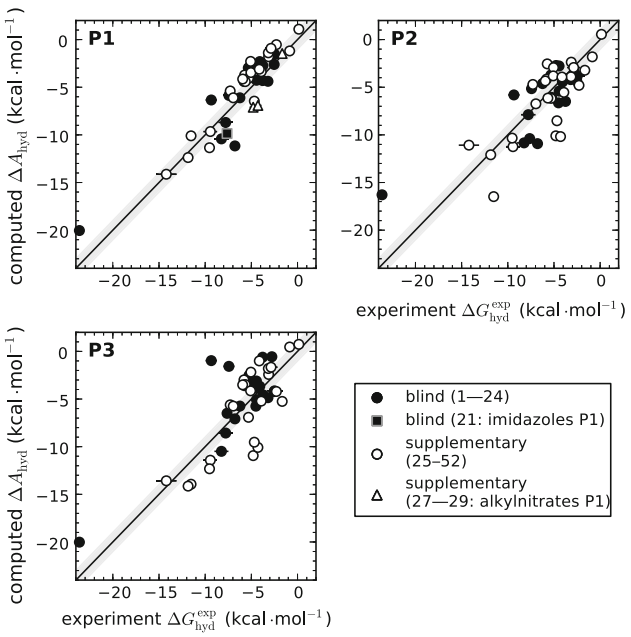

Fig. 4 Correlation between experimental $\Delta G_{\mathrm{hyd}}^{\mathrm{exp}}$ and computed hydration free energies ΔA_{hyd} [see Table 5 for Kendall's tau rank correlation coefficient (τ) and coefficient of determination (R^2) values]. The computed free energy (computed at constant volume) is shown against the experimental value for each parametrization protocol **P1–P3**. Perfect agreement is shown by the diagonal line in each plot and ±1 kcal mol^{-1} from ideal is indicated by the shaded area. *Error bars* denote the experimental or computational error at one standard deviation from the mean. Computational errors are typically smaller than the marker symbols (<0.15 kcal mol^{-1}). Compounds in the blind prediction subset are shown as filled black symbols whereas compounds in the supplementary data set are depicted as empty symbols. Chemical classes of molecules for which new OPLS-AA atom types had to be derived for protocol P1 are highlighted as different symbols as indicated in the legend

our current protocol and reliably predict hydration free energies regardless of the initial conformation of the solute.

Conclusion

Hydration free energies for the SAMPL4 data set were predicted using molecular dynamics simulations with the OPLS-AA force field and three different protocols to generate partial charges to model the electrostatic interactions of the solute with water. The best results were obtained with the transferable OPLS-AA charges (P1) with a RMSE of 1.75 kcal mol^{-1} from experimental data. Non-transferable charges calculated *ab-initio* at the QM level resulted in worse predictions with RMSEs of 2.50 kcal mol^{-1} and 2.76 kcal mol^{-1}, which indicates that the available set of OPLS-AA atom types (including the new parameters introduced here) already covers a reasonable portion of the chemical space required to represent the SAMPL4 compounds. Together with previous results that showed that classical fixed-charge transferable force fields can be made chemically accurate by relatively small interventions, our study suggests that one can expect an accuracy of around 1 kcal mol^{-1} to 2 kcal mol^{-1} from appropriately parametrized transferable OPLS-AA atom types. The simulations suffered from poor reproducibility of the van der Waals component of the free energy, which could be traced back to sensitivity to the initial conditions. Further work is required to understand the underlying source of this effect. In summary, the SAMPL challenges provide an ideal arena to push forward not only computational methods but also to improve existing force fields.

Acknowledgments B.I.I.'s laboratory is a member of the Laboratory of Excellence in Research on Medication and Innovative Therapeutics (LERMIT) supported by a grant from French National Research Agency (ANR-10-LABX-33).

References

1. Nicholls A, Mobley DL, Guthrie JP, Chodera JD, Bayly CI, Cooper MD, Pande VS (2008) Predicting small-molecule solvation free energies: an informal blind test for computational chemistry. J Med Chem 51(4):769–779. doi:10.1021/jm070549+

2. Guthrie JP (2009) A blind challenge for computational solvation free energies: introduction and overview. J Phys Chem B 113(14):4501–4507. doi:10.1021/jp806724u
3. Geballe MT, Skillman AG, Nicholls A, Guthrie JP, Taylor PJ (2010) The SAMPL2 blind prediction challenge: introduction and overview. J Comput Aided Mol Des 24(4):259–279. doi:10.1007/s10822-010-9350-8
4. Geballe MT, Guthrie JP (2012) The SAMPL3 blind prediction challenge: transfer energy overview. J Comput Aided Mol Des 26(5):489–96. doi:10.1007/s10822-012-9568-8
5. Mackerell AD (2004) Empirical force fields for biological macromolecules: overview and issues. J Comp Chem 25(13):1584–1604. doi:10.1002/jcc.20082
6. Jorgensen WL, Tirado-Rives J (2005) Potential energy functions for atomic-level simulations of water and organic and biomolecular systems. Proc Natl Acad Sci USA 102(19):6665–6670. doi:10.1073/pnas.0408037102
7. van Gunsteren WF, Bakowies D, Baron R, Chandrasekhar I, Christen M, Daura X, Gee P, Geerke DP, Glattli A, Hunenberger PH, Kastenholz MA, Oostenbrink C, Schenk M, Trzesniak D, van der Vegt NFA, Yu HB (2006) Biomolecular modeling: goals, problems, perspectives. Angew Chem Int Ed 45(25):4064–4092. doi:10.1002/anie.200502655
8. Helms V, Wade R (1997) Free energies of hydration from thermodynamic integration: comparison of molecular mechanics force fields and evaluation of calculation accuracy. J Comput Chem 18(4):449–462. doi:10.1002/(SICI)1096-987X(199703)18:4<449::AID-JCC1>3.0.CO;2-T
9. Geerke DP, van Gunsteren WF (2006) Force field evaluation for biomolecular simulation: free enthalpies of solvation of polar and apolar compounds in various solvents. ChemPhysChem 7(3):671–678. doi:10.1002/cphc.200500510
10. Mobley DL, Wymer K, Lim NM (2014) Blind prediction of solvation free energies from the SAMPL4 challenge. J Comput Aided Mol Des. doi:10.1007/s1082201497182
11. Shirts MR, Pande VS (2005) Solvation free energies of amino acid side chain analogs for common molecular mechanics water models. J Chem Phys 122(13):134508. doi:10.1063/1.1877132
12. Mobley DL, Dumont E, Chodera JD, Dill KA (2007) Comparison of charge models for fixed-charge force fields: small-molecule hydration free energies in explicit solvent. J Phys Chem B 111(9):2242–2254. doi:10.1021/jp0667442
13. Mobley DL, Bayly CI, Cooper MD, Dill KA (2009) Predictions of hydration free energies from all-atom molecular dynamics simulations. J Phys Chem B 113(14):4533–4537. doi:10.1021/jp806838b
14. Mobley DL, Bayly CI, Cooper MD, Shirts MR, Dill KA (2009) Small molecule hydration free energies in explicit solvent: an extensive test of fixed-charge atomistic simulations. J Chem Theory Comput 5(2):350–358. doi:10.1021/ct800409d
15. Klimovich PV, Mobley DL (2010) Predicting hydration free energies using all-atom molecular dynamics simulations and multiple starting conformations. J Comput Aided Mol Des 24(4):307–316. doi:10.1007/s10822-010-9343-7
16. Sulea T, Corbeil C, Purisima E (2010) Rapid prediction of solvation free energy. 1. An extensive test of linear interaction energy (LIE). J Chem Theory Comput 6(5):1608–1621. doi:10.1021/ct9006025
17. Purisima EO, Corbeil CR, Sulea T (2010) Rapid prediction of solvation free energy. 3. Application to the SAMPL2 challenge. J Comput Aided Mol Des 24(4):373–83. doi:10.1007/s10822-010-9341-9
18. Shivakumar D, Williams J, Wu Y, Damm W, Shelley J, Sherman W (2010) Prediction of absolute solvation free energies using molecular dynamics free energy perturbation and the OPLS force field. J Chem Theory Comput 6(5):1509–1519. doi:10.1021/ct900587b
19. Baker C, Lopes P, Zhu X, Roux B, MacKerell A Jr (2010) Accurate calculation of hydration free energies using pair-specific Lennard-Jones parameters in the CHARMM Drude polarizable force field. J Chem Theory Comput 6(4):1181–1198. doi:10.1021/ct9005773
20. Beckstein O, Iorga BI (2012) Prediction of hydration free energies for aliphatic and aromatic chloro derivatives using molecular dynamics simulations with the OPLS-AA force field. J Comput Aided Mol Des 26(5):635–645. doi:10.1007/s10822-011-9527-9
21. Guthrie JP (2014) SAMPL4, a blind challenge for computational solvation free energies: The compounds considered. J Comput Aided Mol Des (in press)
22. Kaminski G, Duffy E, Matsui T, Jorgensen W (1994) Free energies of hydration and pure liquid properties of hydrocarbons from the OPLS all-atom model. J Phys Chem 98(49):13077–13082. doi:10.1021/j100100a043
23. Jorgensen WL, Maxwell DS, Tirado-Rives J (1996) Development and testing of the OPLS all-atom force field on conformational energetics and properties of organic liquids. J Am Chem Soc 118(45):11225–11236. doi:10.1021/ja9621760
24. Damm W, Frontera A, Tirado-Rives J, Jorgensen W (1997) OPLS all-atom force field for carbohydrates. J Comput Chem 18(16):1955–1970. doi:10.1002/(SICI)1096-987X(199712)18:16<1955::AID-JCC1>3.0.CO;2-L
25. Jorgensen WL, McDonald NA (1998) Development of an all-atom force field for heterocycles. Properties of liquid pyridine and diazenes. J Mol Struct THEOCHEM 424(1–2):145–155. doi:10.1016/S0166-1280(97)00237-6
26. McDonald NA, Jorgensen WL (1998) Development of an all-atom force field for heterocycles. Properties of liquid pyrrole, furan, diazoles, and oxazoles. J Phys Chem B 102(41):8049–8059. doi:10.1021/jp981200o
27. Rizzo RC, Jorgensen WL (1999) OPLS all-atom model for amines: resolution of the amine hydration problem. J Am Chem Soc 121(20):4827–4836. doi:10.1021/ja984106u
28. Kaminski GA, Friesner RA, Tirado-Rives J, Jorgensen WL (2001) Evaluation and reparametrization of the OPLS-AA force field for proteins via comparison with accurate quantum chemical calculations on peptides. J Phys Chem B 105(28):6474–6487. doi:10.1021/jp003919d
29. Watkins EK, Jorgensen WL (2001) Perfluoroalkanes: conformational analysis and liquid-state properties from ab initio and Monte Carlo calculations. J Phys Chem A 105(16):4118–4125. doi:10.1021/jp004071w
30. Price M, Ostrovsky D, Jorgensen W (2001) Gas-phase and liquid-state properties of esters, nitriles, and nitro compounds with the OPLS-AA force field. J Comput Chem 22(13):1340–1352. doi:10.1002/jcc.1092
31. Kony D, Damm W, Stoll S, Van Gunsteren W (2002) An improved OPLS-AA force field for carbohydrates. J Comput Chem 23(15):1416–1429. doi:10.1002/jcc.10139
32. Kahn K, Bruice T (2002) Parameterization of OPLS-AA force field for the conformational analysis of macrocyclic polyketides. J Comput Chem 23(10):977–996. doi:10.1002/jcc.10051
33. Thomas L, Christakis T, Jorgensen W (2006) Conformation of alkanes in the gas phase and pure liquids. J Phys Chem B 110(42):21198–21204. doi:10.1021/jp064811m
34. Jorgensen W, Jensen K, Alexandrova A (2007) Polarization effects for hydrogen-bonded complexes of substituted phenols with water and chloride ion. J Chem Theory Comput 3(6):1987–1992. doi:10.1021/ct7001754
35. Xu Z, Luo HH, Tieleman DP (2007) Modifying the OPLS-AA force field to improve hydration free energies for several amino acid side chains using new atomic charges and an off-plane charge model for aromatic residues. J Comput Chem 28(3):689–697. doi:10.1002/jcc.20560

36. Hess B, Kutzner C, van der Spoel D, Lindahl E (2008) GROMACS 4: algorithms for highly efficient, load-balanced, and scalable molecular simulation. J Chem Theory Comput 4(3):435–447. doi:10.1021/ct700301q
37. Michaud-Agrawal N, Denning EJ, Woolf TB, Beckstein O (2011) MDAnalysis: a toolkit for the analysis of molecular dynamics simulations. J Comput Chem 32:2319–2327. doi:10.1002/jcc.21787
38. Frisch MJ, Trucks GW, Schlegel HB, Scuseria GE, Robb MA, Cheeseman JR, Scalmani G, Barone V, Mennucci B, Petersson GA, Nakatsuji H, Caricato M, Li X, Hratchian HP, Izmaylov AF, Bloino J, Zheng G, Sonnenberg JL, Hada M, Ehara M, Toyota K, Fukuda R, Hasegawa J, Ishida M, Nakajima T, Honda Y, Kitao O, Nakai H, Vreven T, Montgomery JA Jr, Peralta JE, Ogliaro F, Bearpark M, Heyd JJ, Brothers E, Kudin KN, Staroverov VN, Kobayashi R, Normand J, Raghavachari K, Rendell A, Burant JC, Iyengar SS, Tomasi J, Cossi M, Rega N, Millam JM, Klene M, Knox JE, Cross JB, Bakken V, Adamo C, Jaramillo J, Gomperts R, Stratmann RE, Yazyev O, Austin AJ, Cammi R, Pomelli C, Ochterski JW, Martin RL, Morokuma K, Zakrzewski VG, Voth GA, Salvador P, Dannenberg JJ, Dapprich S, Daniels AD, Farkas O, Foresman JB, Ortiz JV, Cioslowski J, Fox DJ (2009) Gaussian ~ 09 Revision D.01. Gaussian Inc., Wallingford CT
39. Jorgensen WL, Chandrasekhar J, Madura JD, Impey RW, Klein ML (1983) Comparison of simple potential functions for simulating liquid water. J Chem Phys 79(2):926–935. doi:10.1063/1.445869
40. Shirts MR, Pitera JW, Swope WC, Pande VS (2003) Extremely precise free energy calculations of amino acid side chain analogs: comparison of common molecular mechanics force fields for proteins. J Chem Phys 119(11):5740–5761. doi:10.1063/1.1587119
41. Essman U, Perela L, Berkowitz ML, Darden T, Lee H, Pedersen LG (1995) A smooth particle mesh Ewald method. J Chem Phys 103:8577–8592. doi:10.1063/1.470117
42. Hess B (2008) P-LINCS: A parallel linear constraint solver for molecular simulation. J Chem Theory Comput 4(1):116–122. doi:10.1021/ct700200b
43. Jorge M, Garrido N, Queimada A, Economou I, Macedo E (2010) Effect of the integration method on the accuracy and computational efficiency of free energy calculations using thermodynamic integration. J Chem Theory Comput 6(4):1018–1027. doi:10.1021/ct900661c
44. Frenkel D, Smit B (2002) Understanding molecular simulations, 2nd edn. Academic Press, San Diego
45. Marenich AV, Kelly CP, Thompson JD, Hawkins GD, Chambers CC, Giesen DJ, Winget P, Cramer CJ, Truhlar DG (2009) Minnesota Solvation Database—version 2009, University of Minnesota, Minneapolis (http://comp.chem.umn.edu/mnsol/)
46. Dror RO, Green HF, Valant C, Borhani DW, Valcourt JR, Pan AC, Arlow DH, Canals M, Lane JR, Rahmani R, Baell JB, Sexton PM, Christopoulos A, Shaw DE (2013) Structural basis for modulation of a G-protein-coupled receptor by allosteric drugs. Nature 503:295–299. doi:10.1038/nature12595